PERGAMON

Neuromuscular Disorders 10 (2000) 121–132

www.elsevier.com/locate/nmd

Integrin and dystrophin associated adhesion protein complexes during regeneration of shearing-type muscle injury

Minna Kääriäinen[a, b], Janne Kääriäinen[a], Teppo L.N. Järvinen[a, b], Liisa Nissinen[c], Jyrki Heino[c], Markku Järvinen[a, b], Hannu Kalimo[d, e,*]

[a]*Medical School and the Institute of Medical Technology, University of Tampere, Tampere, Finland*
[b]*Department of Surgery, Tampere University Hospital, Tampere, Finland*
[c]*Medicity Research Laboratory, Turku, Finland*
[d]*Department of Pathology, Turku University Hospital, Turku, Finland*
[e]*Paavo Nurmi Centre, University of Turku, Turku, Finland*

Received 17 March 1999; received in revised form 25 June 1999; accepted 13 July 1999

Abstract

In shearing injury both the myofibres and connective tissue framework are breached and the muscle–tendon continuity is disrupted. During regeneration the firm myofibre to extracellular matrix (ECM) adhesion must be re-established. We have analysed the expression of selected molecules implementing this adhesion in regenerating myofibres 2–56 days after transection of rat soleus muscle using quantitative immunohistochemistry and Northern blotting. $\beta 1$ integrin mRNA level and $\alpha 7$ integrin and vinculin immunoreactivities were transiently increased in both the intact and regenerating parts of the transected myofibres by day 5–7 with normalization by day 10–14. After day 14, $\alpha 7$ integrin and vinculin accumulated at the tips of the regenerating myofibres, indicating formation of new mini-myotendinous junctions (mMTJ). Immunoreactivities for dystrophin and associated proteins as well as merosin appeared in regenerating myotubes by day 3–4 reaching control levels by day 56. Our results suggest that integrin and dystrophin associated molecules are complementary in myofibre-ECM adhesion. During regeneration, ruptured myofibres temporarily reinforce their integrin mediated lateral adhesion until mMTJs are formed. Thereby the load on the newly formed scar and the risk of rerupture are reduced. Dystrophin associated molecules appear later and replace integrin on the lateral aspects, while both complexes are abundant at the mMTJs. These molecular events correspond to our previous results on tensile strength.

Keywords: Muscle regeneration; Adhesion; $\alpha 7$ integrin; $\beta 1$ integrin; Vinculin; Dystrophin; β-dystroglycan; α-sarcoglycan; Merosin

1. Introduction

In our previous study, we developed a muscle injury model, in which unipennate muscle, rat soleus, is transected, and determined the restoration of tensile strength in relationship to histopathological changes during the natural course of the muscle repair process [1]. In this shearing type of injury [2] not only the myofibres but also their basement membrane (BM) and the mysial sheaths are transected which causes a disruption of the functional continuity of the muscle–tendon complex. Optimal repair necessitates a balanced interaction between the regenerating muscle cells and extracellular matrix (ECM). On one hand, the proximal and distal stumps of the transected myofibres must restore their structural integrity and, on the other hand, the regenerating myofibres must also bind firmly to the ECM to re-establish the functional continuity.

The adhesion of myofibres to the surrounding ECM is accomplished by two main complexes of adhesion molecules, integrin and dystrophin associated, which connect the contractile proteins of sarcomeres to laminin in the BM, reviewed in [3–9]. In the integrin associated complex, sarcomeric actin binds via several subsarcolemmally located molecules, such as α-actinin, talin, vinculin, paxillin and tensin to the $\beta 1$ subunit of the muscle specific [10] integrin $\alpha 7\beta 1$ [4,11–13]. Integrin $\alpha 7\beta 1$ is enriched in the myotendinous junction (MTJ) with only minor amounts being present on the lateral aspects of the myofibre plasma membrane [14]. Integrin $\alpha 7\beta 1$ is a receptor for merosin, the muscle specific laminin-2 [15–18].

In the dystrophin associated complex, actin binds to subsarcolemmally located dystrophin [19–25], which is

* Corresponding author. Dr. Hannu Kalimo, Department of Pathology, Turku University Hospital, Kiinamyllynkatu 10, FIN-20520 Turku, Finland. Tel.: +358-2-2611685; fax: +358-2-3337459.
E-mail address: hkalimo@utu.fi (H. Kalimo)

0960-8966/00/$ - see front matter
PII: S0960-8966(99)00077-2

also enriched in MTJs and neuromuscular junctions (NMJ) [26–29]. Dystrophin is associated with three protein complexes [30–33], dystroglycans, sarcoglycans and syntrophins [34]. Dystrophin binds with its C-terminus to the transmembrane β-dystroglycan (β-DG) [35,36], which is linked to the extracellular α-dystroglycan (α-DG) [34]. α-DG in turn binds to merosin in the BM [37,38]. The transmembrane α-, β-, γ- and δ-sarcoglycans associate with dystrophin but their role in mediating the interaction with extracellular molecules is not yet understood [32,34].

The purpose of this study was to investigate the re-establishment of integrin and dystrophin associated adhesion during the regeneration process following shearing type of skeletal muscle injury. Results were correlated with the biomechanical and histopathological changes reported in our previous study [1].

2. Materials and methods

2.1. Animals and muscle injury

Seventy two adult male Sprague–Dawley rats were used in this study. The average age at the time of traumatization was 12 weeks and the body weight 413 g. The animals were housed in cages and fed with commercial pellets and water ad libitum. The research protocol was accepted by the ethical committee for animal experiments of the University of Tampere.

Animals were randomly divided into ten subgroups on the basis of the postinjury interval (see below, $n = 8$ in each subgroup, except for those of days 2 and 4 in which $n = 4$), each including bilaterally and unilaterally traumatized animals. Animals were anaesthetized with an intraperitoneal injection of pentobarbital (Mebunat; Orion-Farmos, Turku, Finland) solution. Under anaesthesia, a longitudinal incision was made along the lateral aspect of either right or both calves (unilateral or bilateral trauma). The soleus muscle was gently exposed avoiding detaching it from the surrounding fascia. Thereafter, the soleus muscle was completely transected with microscissors in a transverse plane (Fig. 1). The stumps were covered and kept aligned by suturing (Vicryl; Johnson & Johnson Ethicon, Norderstedt, Germany) the overlying fascia and finally, the skin was closed. The contralateral intact limbs of the unilaterally traumatized animals served as controls. Postoperatively animals were allowed to move freely in the cages. Animals were sacrificed 2, 3, 4, 5, 7, 10, 14, 21, 28 and 56 days postoperatively with an overdose of carbon dioxide.

2.2. Histology and immunohistochemistry

The muscle samples were collected and frozen in isopentane cooled with liquid nitrogen. Longitudinal frozen sections were stained with hematoxylin & eosin (H&E) and Herovici for morphological examinations. Immunohistochemistry was performed with mouse monoclonal antibodies to the following molecules: α7 integrin (a kind gift from Dr Stephen Kaufman, University of Illinois, Urbana, IL) and vinculin (Serotec Ltd, Oxford, UK), and dystrophin 2, β-DG, α-SG and merosin (all from Novocastra, Newcastle, UK). The bound antibodies were visualized using avidin-biotin peroxidase kit (Vectastain, Vector Laboratories, Burlingame, CA) with diaminobenzidine as the chromogen and hematoxylin as the counterstain.

2.3. Quantification of immunohistochemistry

The maximal intensity (relative optical density, ROD) of the immunoreactivity associated with the plasma membrane or BM was measured using Microcomputer Imaging Device version M4 (Imaging Research Inc., Brock University, St. Catharines, Ontario, Canada). Measurements were performed on captured digital pictures by scanning the intensity of immunopositivity in a band of selected width, which is perpendicular to the plasma membrane and BM (Fig. 2). In addition, the staining of sarcoplasm was measured. Measurements in each sample were made in ten different areas.

The intensity of immunoreactivity was measured in each traumatized muscle sample both in the regenerating part (i.e. in the regeneration and central zones, (RZ and CZ), see Fig. 1) and intact part of the muscle (i.e. in the survival zone, (SZ) see Fig. 1). Corresponding intensity was also measured in sections from the contralateral intact control muscle of the unilaterally traumatized animals, which were immunostained on the same slide with sections from

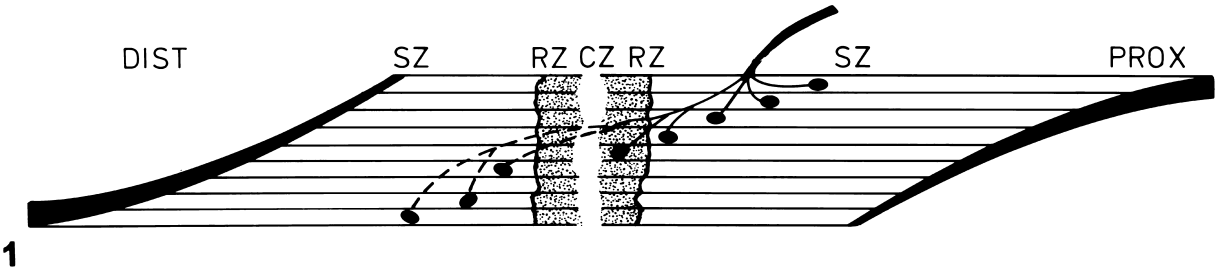

Fig. 1. A schematic illustration of the injury. Soleus is a unipennate muscle, in which all myofibres extend parallelly from the proximal to the distal tendon. The muscle was cut transversely slightly distal to the point where the nerve enters the muscle belly. For definitions of the three zones, central zone (CZ), regeneration zone (RZ) and survival zone (SZ) see Section 3.

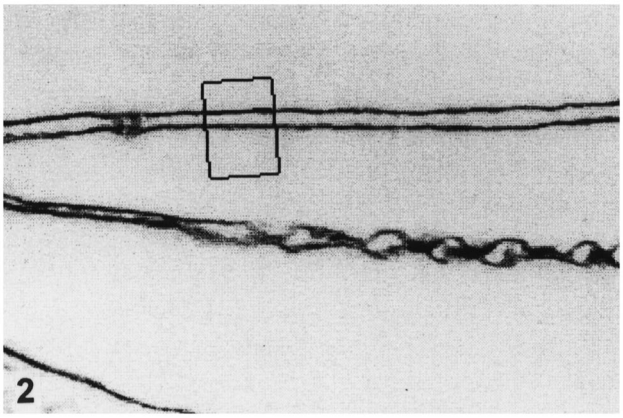

Fig. 2. A captured picture of myofibres stained with dys-2 antibody. The square exemplifies the area within which the intensity of the immunoreactivity was measured as an average over the range of plasma membrane or BM perpendicularly cross the myofibre.

the traumatized muscle. The intensity of immunoreactivity of each molecule in the RZ and CZ of the regenerating myofibres was expressed as a percentage of the intensity in intact muscle, i.e. in either SZ or control muscle.

Average value of the non-specific staining of sarcoplasm in the intact area was used as the backround error value (BEV). The BEV in the same section was subtracted from the average intensity of immunostaining of the plasma membrane or BM in both the regenerating and intact area (see formula). The formula of the calculation used was:

$$\text{Intensity of true immunoreactivity (\%)} = 100 \times (\text{ROD}_{\text{regeneration}} - \text{BEV}_{\text{intact}})/(\text{ROD}_{\text{intact}} - \text{BEV}_{\text{intact}}).$$

$\text{ROD}_{\text{intact}}$ represents the intensity of immunoreactivity either in the SZ of the same tissue section (for dystrophin and associated molecules) or in a control section from the contralateral muscle immunostained on the same slide (for integrin associated molecules). Contralateral intact muscles had to be used as reference values for the integrin associated molecules because a trauma induced upregulation occurred in the SZ.

The reproducibility of the quantification of immunohistochemistry by image analysis was determined by comparing data from two repeated measurements on 28 different immunohistochemical sections of dystrophin staining. Reproducibility was defined as the 95% limit of agreement for the differences observed in repeated measurements (i.e. average bias ± twice the standard deviation of the differences) [39]. The 95% limit of agreement was used as a measure of reproducibility in order to make certain that the observed differences during the observation period of 56 days were significantly larger than those occuring by chance.

2.4. Data analysis

Analysis of variance (ANOVA), followed by Bonferroni correction for multiple comparisons, was performed for each molecule to compare the intensity of immunostaining between different time points of regeneration. Analysis of variance, using subject, i.e. rat as a random factor, was also used to compare the intensity of immunostaining between different molecules at each healing time point.

2.5. RNA extractions and Northern blot hybridizations

Total cellular RNA was isolated using the guanidium thiocyanate/CsCl method [40]. 20 μg of total cellular RNA was separated in formaldehyde-containing 1% agarose gels, transferred to nylon membranes (ZETA-probe, Biorad), and hybridized with ^{32}P-labelled (Amersham) cDNAs for rat $\alpha 1$ (I) collagen [41], rat $\beta 1$ integrin, rabbit dystroglycan [37] and rat glyceraldehyde-3-phosphate dehydrogenase (GAPDH; a ''house keeping'' enzyme used as a control) [42] probes. Dystroglycan cDNA was a kind gift from Dr Kevin Campbell (Iowa City, IA). Rat $\beta 1$ integrin cDNA corresponding to nucleotides 45–994 (unpublished sequence in Gene Bank, accession number U12309) was amplified by RT-PCR using total RNA isolated from rat granulation tissue cells. Autoradiograms were quantified with Microcomputer Imaging Device version M4 (see above), and results corrected for GAPDH mRNA levels.

3. Results

3.1. Histology

The histopathological pattern of regeneration after this shearing type of injury followed the same scheme as described previously in detail [1,43,44]. In short, immediately after injury the myofibre stumps retracted and the gap between them formed the central zone (CZ, Fig. 1). This was first filled by a haematoma, which was later replaced by connective tissue. Myofibres became necrotized from the site of transection over a distance of 1–2 mm inside their preserved BM cylinders. In the next stage the new demarcation membrane limited the extension of necrosis and delineated the regeneration zone (RZ) from the survival zone (SZ), where myofibres survive with certain reactive changes (Fig. 1).

By day 2 satellite cells had proliferated and become myoblasts. On day 3 the myoblasts had begun to fuse to form myotubes. By day 5 these had filled the old BM cylinders in the RZ up to the boundary between the RZ and the CZ. On day 7 the tips of the regenerating myotubes extended from the BM cylinders into the connective tissue of the CZ, attempting to pierce through the scar. Maturation of myotubes into myofibres had commenced by day 14, when cross-striation was already visible. From day 14

onwards the connective tissue of the CZ contracted and continuously decreased in amount. Thereby the stumps with newly formed mMTJs at their tips were pulled closer to each other and they became more interlaced and better organized. Yet, even on day 56 the stumps remained separated by a thin layer of scar tissue (cf. Fig. 5C).

3.2. Immunohistochemistry

3.2.1. α7 integrin and vinculin in intact parts of injured myofibres (in the SZ)

In the control muscles, strong immunoreactivities for α7 integrin and vinculin were observed in MTJs (not shown), whereas the plasma membranes stained very faintly (Fig. 3A). Remarkably, intact parts of the myofibres in the SZ showed strong increases in the intensity of immunoreactivities for α7 integrin (Figs. 3B and 4A) and vinculin (Figs. 3C and 4B) in the plasma membrane from day 4 onwards. The increase in intensity of α7 integrin was similar along the whole length of the myofibres in the SZ reaching its peak of about 170–180% of that in the contralateral intact soleus on day 7 (Fig. 4A). Thereafter, the intensity rapidly returned to normal levels by day 10. The increase in the intensity of vinculin immunoreactivity in the SZ displayed a clear gradient along the injured myofibre and it was most marked next to the injury site reaching a maximum of 186% on day 7 (Fig. 4B). Close to the MTJs in the proximal and distal SZ, i.e. farthest away from the lesion, the maximum increase was only 117% on day 5 (Figs. 3D and 4B).

3.2.2. α7 integrin and vinculin in regenerating parts of injured myofibres (in the RZ and CZ)

On day 3 after the injury, the immunoreactivity for α7 integrin was mainly localized to the cytoplasm of regenerating myotubes in the RZ as granular staining with accentuation close to the plasma membrane. Cytoplasmic staining was still relatively strong during days 4–7, but by day 14 it had more or less completely disappeared. Cytoplasmic staining for vinculin was not measurable either on day 3 or later during the muscle regeneration process.

Immunostaining of the plasma membrane for α7 integrin in the RZ was weak and focal on day 3, but it became progressively more intense (Figs. 5A and 6) increasing from 86% on day 3 to a maximum of 175% on day 7 (Fig. 6). Thereafter the immunoreactivity along the lateral

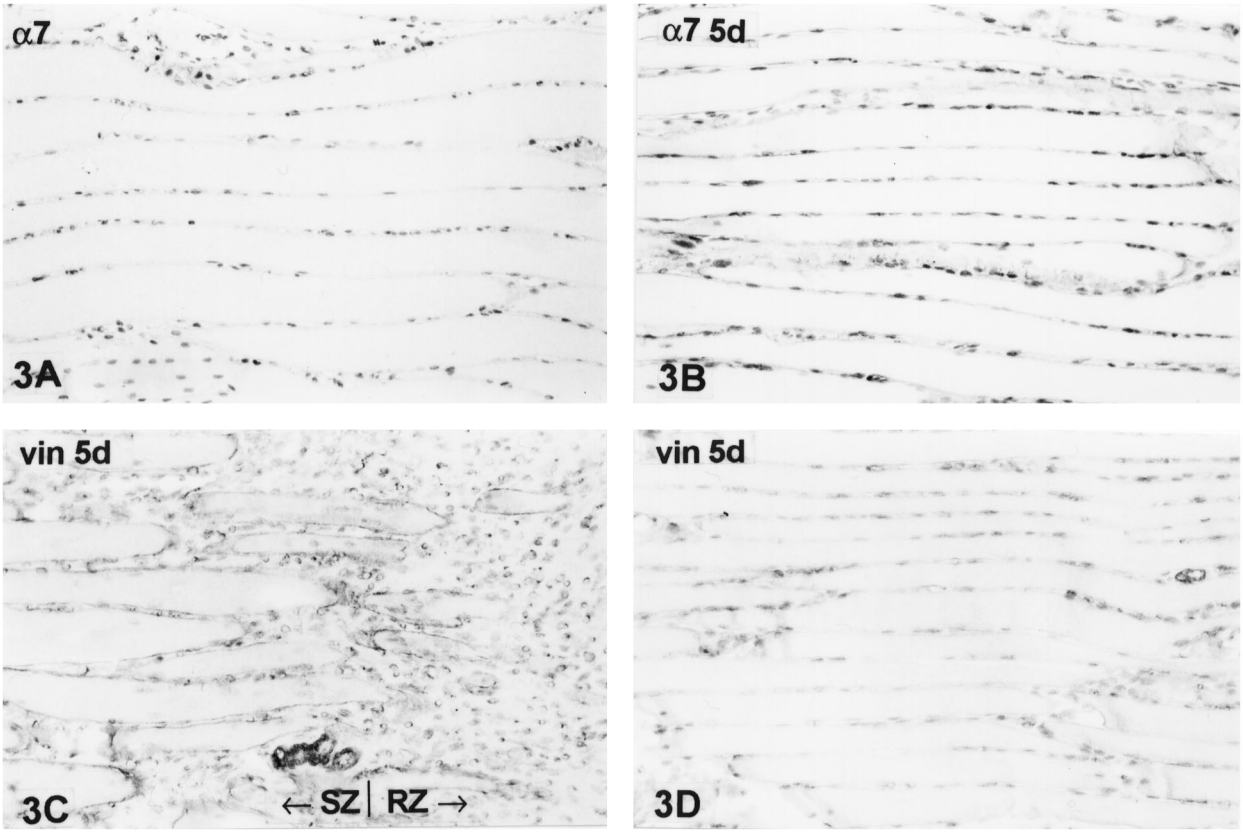

Fig. 3. (A) In the contralateral non-lesioned control muscle the immunoreactivity along the sides of myofibres is very weak for α7 integrin. (B) In the intact part of the transected myofibres (i.e. in the SZ) the intensity of α7 integrin immunoreactivity on day 5 is clearly increased (cf. Fig. 4A) as compared to the control muscle. (C) In the proximal SZ (close to the RZ) the intensity of vinculin immunoreacivity is clearly increased on day 5 (cf. Fig. 4B). (D) In the distal SZ (distant to the RZ) the intensity of vinculin immunoreactivity is similarly weak as for α7 integrin in the control muscle. Immunoperoxidase with haematoxylin counterstaining. ×115.

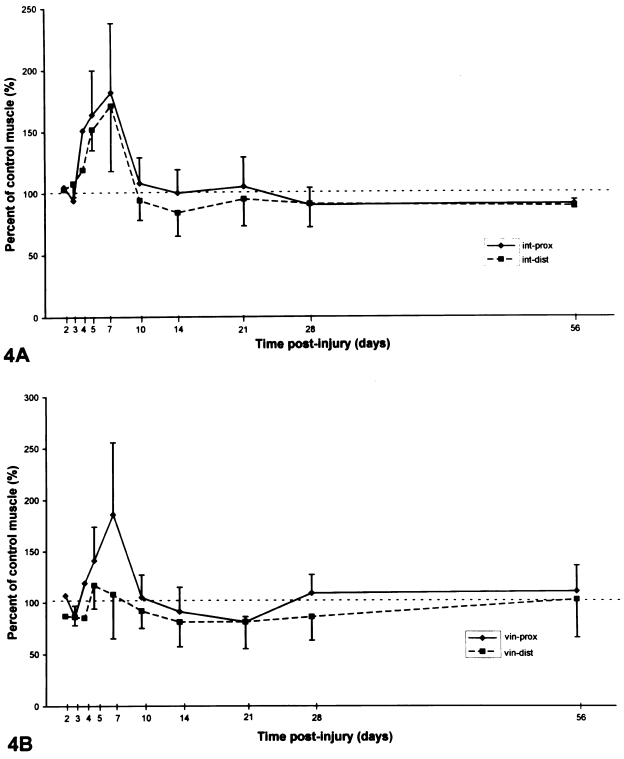

Fig. 4. The intensities of α7 integrin (A) and vinculin (B) immunoreactivities ($\pm$SD) in the SZ close to (prox) and distant to (dist) the injury. The results are expressed as percentages of the control values in the intact contralateral muscles. Immunoreactivity for α7 integrin on day 7 differed significantly from days 3 and 10–56 ($P < 0.01$) and immunoreactivity on day 5 from days 3, 14, 28 and 56 in the proximal part of the SZ ($P < 0.05$) and from days 10–56 in the distal part of the SZ ($P < 0.05$) (ANOVA). Immunoreactivity for vinculin on day 7 differed significantly from days 3, 14 and 21 ($P < 0.01$) and from days 10, 28 and 56 ($P < 0.05$).

aspects returned to control levels by day 14, whereas at the tips of the regenerating myofibres it became accentuated suggesting formation of new mMTJs (Fig. 5B,C)

The pattern of changes in the intensity of vinculin immunoreactivity was very similar (Figs. 5C and 6), but the increase for vinculin was more rapid, somewhat greater (maximum 241% on day 5), and lasted longer than for α7 integrin (Fig. 6). After day 5 the immunoreactivity returned to control levels by day 28. Vinculin immunoreactivity also became accentuated at the tips of the regenerated myofibres.

On day 56 the staining patterns for α7 integrin and vinculin were compatible with an independent adhesion of the proximal and distal stumps of the regenerated myofibres to the intervening connective tissue instead of becoming fused with each other (Fig. 5C).

3.2.3. Dystrophin, β-dystroglycan and α-sarcoglycan

In the control muscles, the immunoreactivities for dystrophin (Fig. 7A) and the two associated proteins, β-DG and α-SG (data not shown) were identified as a distinct, continuous line delineating the plasma membrane. The intensities of their immunostaining in the SZ of regenerating myofibres remained similar to that in control sections throughout the observation period.

Immunoreactivities for these three molecules were not seen in the RZ until the regeneration had progressed to the

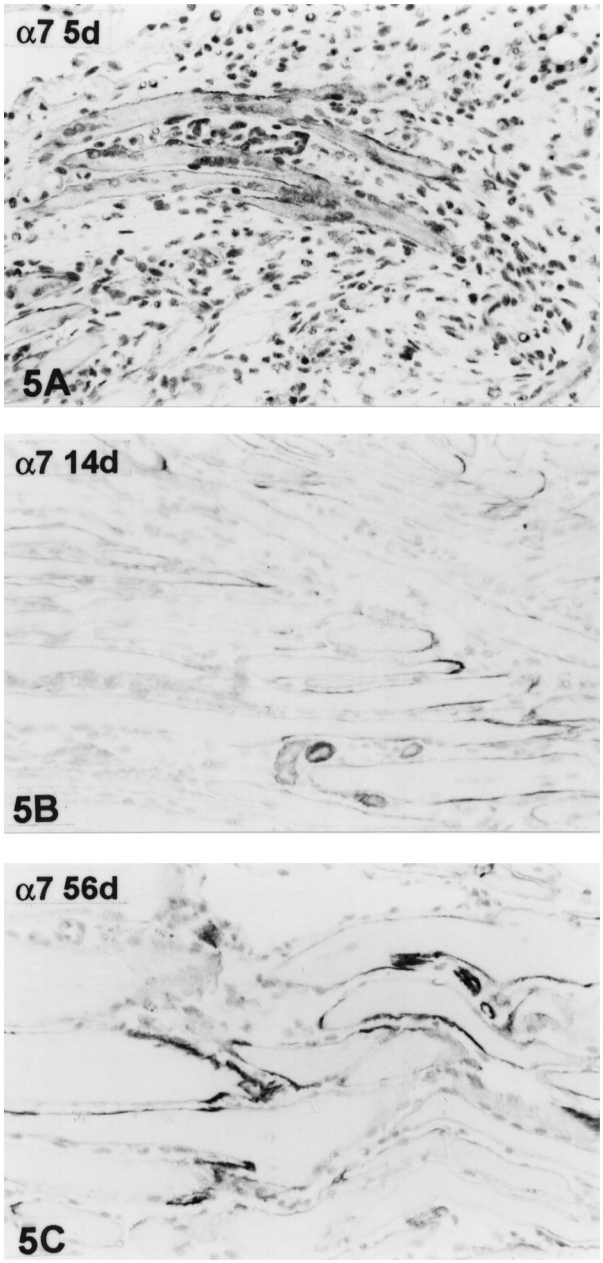

Fig. 5. (A) On day 5, the intensity of α7 integrin immunoreactivity on the plasma membrane of the regenerating myotubes (i.e. in the RZ) is clearly increased (cf. Fig. 6) as compared to the control muscle. (B) On day 14, α7 integrin immunopositivity on the regenerating myofibres in the RZ shows focal accentuations indicating clustering and incipient formation of mMTJs. The stumps have become interlaced due to contraction and resorbtion of the interposed scar tissue. (C) On day 56, the new mMTJs are clearly seen as foci of accentuated α7 integrin immunoreactivity. Further away from the tips of regenerating myofibres the intensity of α7 integrin immunoreactivity is weaker. The results for vinculin were identical to these for α7 integrin (data not shown). Immunoperoxidase and haematoxylin counterstaining. ×180.

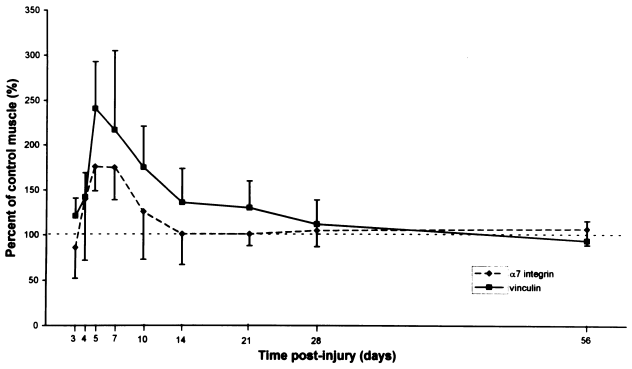

Fig. 6. The intensities of $\alpha 7$ integrin and vinculin immunoreactivities ($\pm$SD) in the RZ. The results are expressed as percentages of the control values in the intact contralateral muscles. Immunoreactivities for $\alpha 7$ integrin on days 5 and 7 were significantly stronger compared to day 10 ($P < 0.05$) and days 3 and 14–56 ($P < 0.01$) (ANOVA). Immunoreactivity for vinculin on day 5 differed significantly from days 3, 4 and 14–56 ($P < 0.01$) and immunoreactivity on day 7 from day 14 ($P < 0.05$) and days 21–56 ($P < 0.01$).

myotube stage, for β-DG and α-SG on day 3 and for dystrophin on day 4. At the early stage immunoreactivities also appeared in the cytoplasm of myotubes as granular staining often located close to the plasma membrane and the immunodecoration of plasma membranes was irregular, indicating that much of these proteins had not yet been incorporated to the plasma membrane. The cytoplasmic immunoreactivities tapered off after day 5 and disappeared by days 10, 14 and 5 for dystrophin, β-DG and α-SG, respectively, to leave only very weak diffuse background positivity.

Even though the onset of dystrophin expression was slightly delayed compared to that of β-DG and α-SG, it was ahead of them after day 5 with α-SG being the slowest to recover (Figs. 7B–E and 8). The dystrophin immunoreactivity on the plasma membrane in the RZ and CZ rapidly increased and reached a 50% level of the corresponding intensity in the SZ by approximately 8 days. β-DG and α-SG did not reach 50% level until days 17 and 22, respectively. By the end of the observation period on day 56, the differences between intensities of dystrophin, β-DG and α-SG immunoreactivities had disappeared, with all of them having almost reached the control values, i.e. 92, 95 and 85%, respectively (Fig. 8). The relative intensity of the dystrophin immunoreactivity was significantly greater than that of β-DG on days 10, 14 ($P < 0.01$) and 21 ($P < 0.05$), and that of α-SG on days 7–28 (ANOVA). The β-DG immunoreactivity also differed significantly from α-SG on day 28 ($P < 0.05$).

3.2.4. Merosin

The merosin antibody stained the BM in both the control muscles (Fig. 9A) and in the SZ of injured myofibres similarly as a distinct continuous line throughout the observation period. Because the BM in the RZ around the necrotized part of the transected myofibres is not phagosytosed, the merosin antibody persistently stained the preserved, old corrugated BM (Fig. 9B), in contrast to the early negative immunostaining for $\alpha 7$ integrin, vinculin, dystrophin, β-DG and α-SG. The first sign of the formation of new BMs around the regenerating myofibres appeared on days 4–5, when weak merosin immunoreactivity was detected inside the old BMs in the RZ. Between days 5 and 21 the expression of merosin was parallel to that of β-DG, reaching an intensity of 50% approximately on day 17 (Figs. 9C and 8). After day 21, the increase in merosin immunoreactivity was slower, reaching an intensity of 82% by day 56. The relative intensity of the merosin immunoreactivity was significantly weaker compared to that of dystrophin on days 7 ($P < 0.05$), 10, 14 and 28 ($P < 0.01$) (ANOVA). In addition, it differed significantly from that of β-DG on day 28.

3.3. Reproducibility of the quantification of immunohistochemistry

The mean difference of the repeated measurements was 3.9% and the SD of the differences was 11.2%. Therefore, the calculated 95% limits of agreement for the repeated measurements by image analyser were 26% and 19%.

3.4. Northern blot analysis

The mRNA levels of $\alpha 1$(I) collagen, $\beta 1$ integrin and dystroglycan measured by Northern blot hybridizations are illustrated in Fig. 10a. Collagen $\alpha 1$(I) mRNA levels were very low in normal muscle but there was a huge upregulation (more than 150-fold) by day 7 (Fig. 10b). The levels were back to control on day 28. These observations were in accordance with those we published previously [45,46]. Integrin $\beta 1$ mRNA levels were upregulated about 4-fold by day 5 and returned to control levels by day 10, indicating a response that was faster and more transient than that for $\alpha 1$(I) collagen (Fig. 10b). Corresponding to the slow increase in the immunoreactivities for dystrophin associated molecules no early rise in dystroglycan mRNA levels occurred, instead the changes were relatively small during the healing process.

4. Discussion

4.1. General aspects

Shearing injury is the most common and, thus, clinically most important type of muscle injury [2]. In shearing injury the connective tissue sheaths are also ruptured in contrast to the in situ necrosis type of muscle injury in which the myofibres are necrotized within their intact BM. Consequently, the regeneration process in shearing injury is more complicated, because regenerating myofibres must also re-estab-

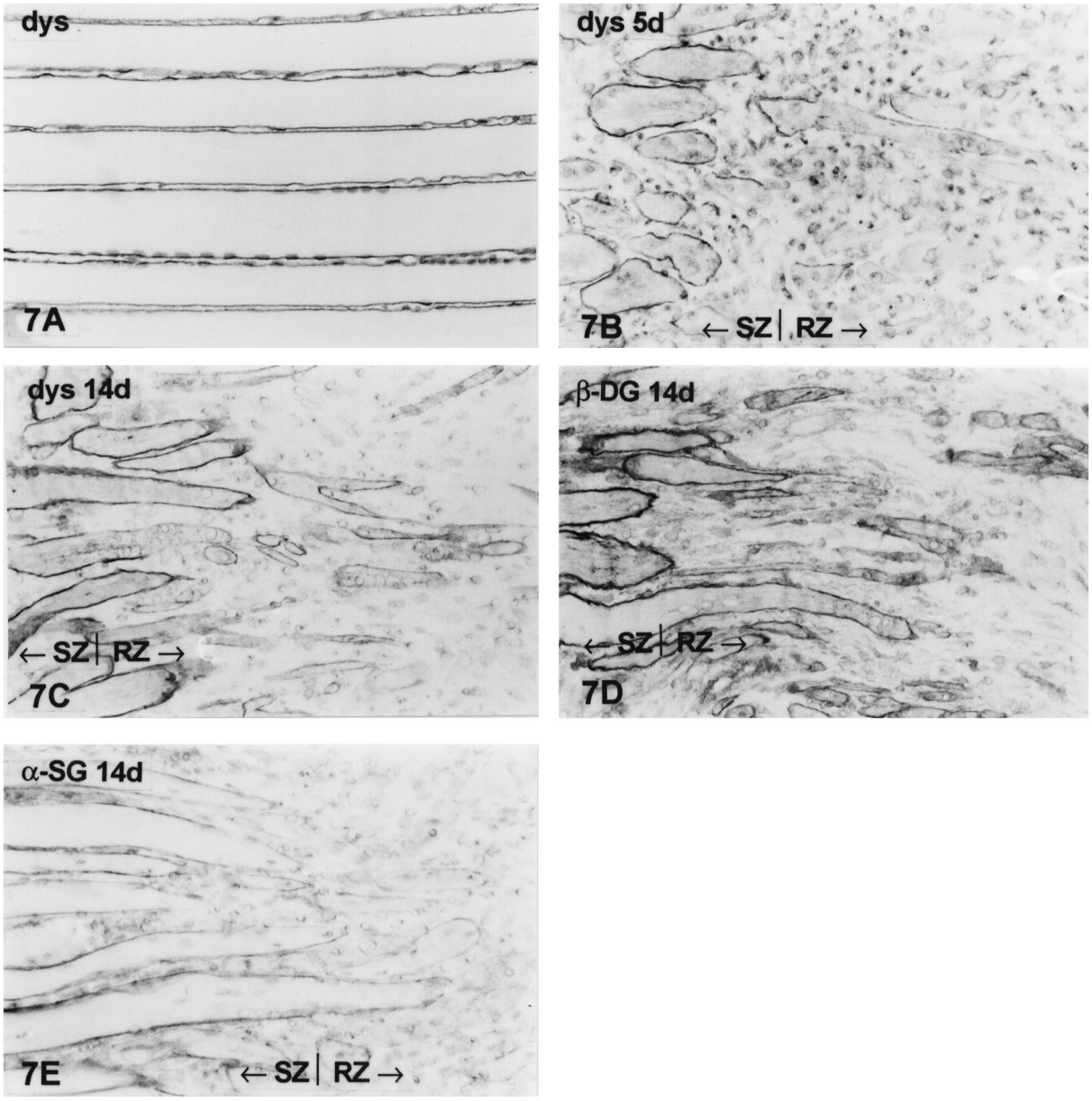

Fig. 7. (A) In the non-lesioned control muscle the dys-2 antibody delineates the myofibres by a strongly immunoreactive line. (B) On day 5, the dys-2 immunoreactivity is just barely visible in the RZ. C–E: On day 14, immunoreactivity with dys-2 antibody has reached over 60% of the control intensity (C), immunoreactivity for β-DG is about 45% of the control intensity with more diffuse staining pattern (D) and immunoreactivity for α-SG has increased most slowly being about 35% (E). (Cf. Fig. 8). Immunoperoxidase with haematoxylin counterstaining. ×180.

lish their attachment to the ECM. Integrin and dystrophin associated complexes of adhesion molecules are pivotal in the implementation of this attachment by connecting the contractile proteins of sarcomeres to the extracellular connective tissue, reviewed in [3–9]. These complexes have to bear extensive loads during the muscle contraction when they transform the force generated by the contractile proteins to movement [47,48]. Therefore, the restitution of these molecular complexes during the muscle regeneration process is essential for restoring the tensile strength of injured muscle.

4.2. Reliability of the quantification of results

Quantitative immunohistochemistry is the only method which allows analysis of the expression of the integrin and dystrophin associated molecules at their functional site, i.e. being associated with the plasma membrane and connecting the cytoskeleton to the ECM. It was also deemed important to assess changes in all three zones of regeneration (i.e. CZ, RZ and SZ, Fig. 1A) so as to fully understand the process. The immunohistochemical analyses were complemented by Northern blotting analysis of one repre-

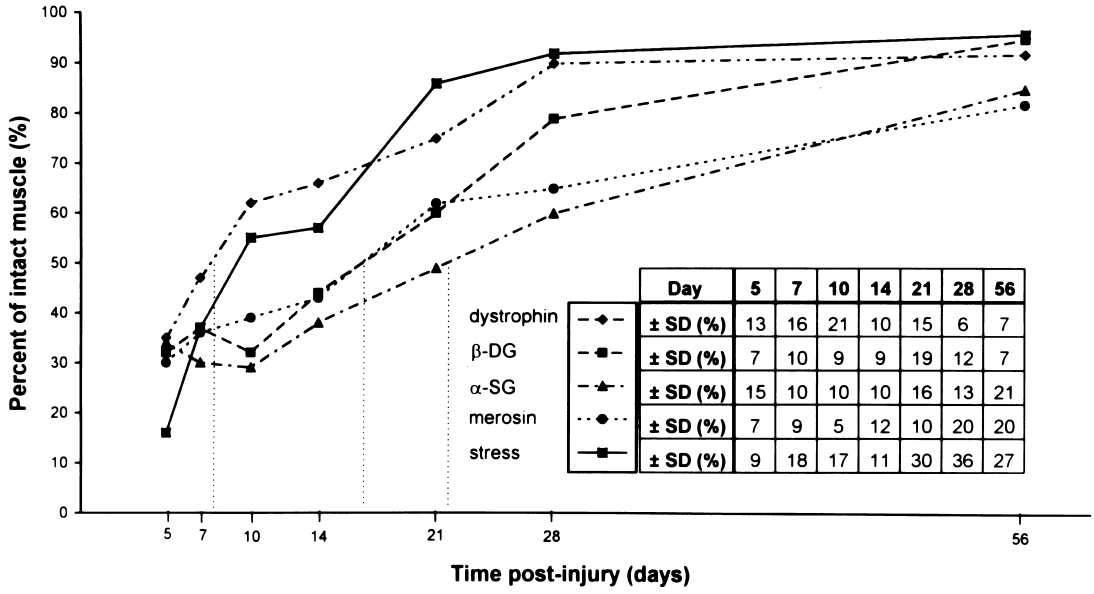

Day	5	7	10	14	21	28	56
± SD (%)	13	16	21	10	15	6	7
± SD (%)	7	10	9	9	19	12	7
± SD (%)	15	10	10	10	16	13	21
± SD (%)	7	9	5	12	10	20	20
± SD (%)	9	18	17	11	30	36	27

Fig. 8. The intensities of dystrophin, β-DG, α-SG and merosin immunoreactivities in the RZ. The results are expressed as percentages of corresponding immunoreactivities in the SZ of the same tissue section. For correlation the increase in the stress (force per physiological cross-sectional area) is also given. Standard deviations are given in the inset table. Immunoreactivity for dystrophin on day 5 was significantly weaker compared to day 10 ($P < 0.05$) and days 14–56 ($P < 0.01$) and day 7 differed from days 21–56 ($P < 0.01$) (ANOVA). Immunoreactivities on days 10 ($P < 0.01$) and 14 ($P < 0.05$) were also significantly weaker compared to days 28 and 56. Immunoreactivity for β-DG on days 5–10 was significantly weaker compared to days 21–56 ($P < 0.01$). In addition, days 14 ($P < 0.01$) and 21 ($P < 0.05$ and $P < 0.01$) differed significantly from days 28 and 56. Immunoreactivities for α-SG on day 5 ($P < 0.05$) and on days 7 and 10 ($P < 0.01$) were significantly weaker compared to day 28. In addition, days 5–21 ($P < 0.01$) and 28 ($P < 0.05$) differed significantly from day 56. Immunoreactivity for merosin on days 5–14 was significantly weaker compared to day 56 ($P < 0.01$). Days 5 and 7 ($P < 0.01$) and 10 ($P < 0.05$) also differed significantly from day 28 and day 5 ($P < 0.01$) from day 21.

sentative molecule of each complex, i.e. β1 integrin and dystroglycan.

We emphasize that the intensities of the immunoreactivities were measured with an image analyser and quantified as a relative value (%) of the internal standard on the same microscopic slide, for dystrophin and associated molecules in the SZ of the lesioned muscle, and for α7 integrin and vinculin in the section from the contralateral non-lesioned muscle of the same unilaterally traumatized animal. The latter standard was needed, because the intensities of α7 integrin and vinculin immunoreactivities in the SZ of regenerating myofibres were significantly increased (for the biological significance, see below), whereas those of dystrophin and associated molecules as well as merosin remained at the control level. Even though the exact relationship between the level of expression and the intensity of immunoreactivity for each molecule is not known, the relative (percentile) intensities give a reliable estimate of the accumulation of each molecule as evidenced by the high statistical significances reached for this accumulation (see the legends of Figs. 4, 6 and 8). Similarly, even if the relationship between the amount of protein and intensity of immunoreactivity were not linear, our analysis gives a fairly good estimate of the rates of accumulation of different molecules, because we made the comparisons between the relative (not absolute) intensities of each molecule at different time points. The statistical analysis revealed that the reproducibility of these quantifications was good, considering the marked intensity changes.

4.3. α7 integrin and vinculin in regenerating parts of injured myofibres (in the RZ and CZ)

The α7 integrin subunit forms a heterodimer with β1 integrin. The formation of this α/β complex in the endoplasmic reticulum seems to be critical in the transport of the β1 integrins to the cell surface [49]. Our analysis of the steady state levels of β1 integrin mRNA demonstrated a maximal increase in the regenerating parts (in the RZ and CZ) before day 5. This indicates that the upregulation of integrin expression is faster and at the same time more transient than for example the stimulation of collagen synthesis in the adjacent scar tissue. Correspondingly, α7 integrin and vinculin immunoreactivities appeared in the plasma membrane of the regenerating parts of the myofibres early, reaching their maximal intensities already at the myotube stage around days 5–7. Apparent, although non-quantified, increases in the immunoreactivities for β1 integrin [50] and vinculin [51] have been previously reported in regenerating myofibres after contusion injury of muscle.

The normalization of α7 integrin and vinculin immunoreactivities over the lateral aspects and their accentuation at

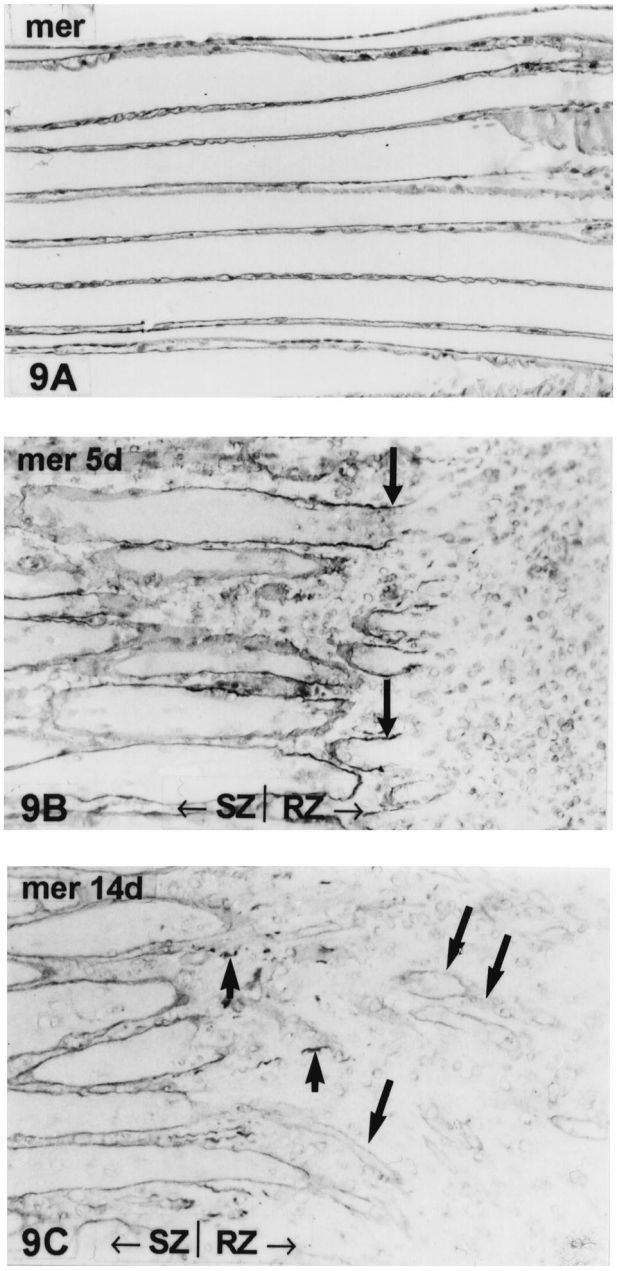

Fig. 9. (A) Intact myofibres in non-lesioned control muscle are surrounded by merosin immunoreactive rim of BM. (B) By day 5 the old BM in the RZ is depicted by slightly corrugated immunoreactivity for merosin, that is often open towards the CZ (arrows). Within this BM cylinder there are numerous nuclei of proliferated myogenic cells. (C) By day 14 the old BM cylinders in the RZ have become fragmented (short arrows) and the regenerating myotubes have become surrounded by newly formed BM (three marked with a long arrow). Immunoperoxidase with haematoxylin counterstaining. (A,B) ×115; (C) ×180.

the tips of the regenerating myofibres began around day 14, at which time the regenerating fibres have extended out of the old BM cylinders and penetrated into the scar tissue between the stumps. Remarkably, this timing coincides with the formation of new mMTJs at the tips of the regenerating myofibres as previously demonstrated by our group [43]. It is conceivable that when regenerating myofibres are still growing into the scar tissue their tips cannot yet be firmly attached and instead they reinforce their lateral binding. Later, when the outgrowth ceases and firm adhesion is required, $\alpha 7$ integrin and vinculin molecules most likely move along the plasma membrane to new mMTJs at the tips of the regenerating myofibres, and consequently lateral immunopositivity decreases. In fact, Felsenfeld et al. recently described such lateral movement of $\beta 1$ integrins along cell surface, possibly guided by ligand binding [52].

4.4. $\alpha 7$ integrin and vinculin in intact parts of injured myofibres (in the SZ)

We found an early and rapid increase in the intensities of $\alpha 7$ integrin and vinculin immunoreactivities not only in the regenerating part (in the RZ and CZ) but also in the intact part of the injured myofibre in the SZ with similar magnitude and timing as in the RZ and CZ. It may be speculated that injury signals for intensified lateral adhesion from the regenerating part of the myofibre into the intact part in the SZ. By means of this extension, the surface area for integrin associated adhesion becomes vastly larger. Functionally this may be very important, because lateral adhesion strengthens the binding between regenerating myofibres and the surrounding ECM (see Section 4.6). Similarly as in the RZ, the intensity of lateral immunoreactivity decreases in the SZ, when the reinforced lateral adhesion is no longer needed after formation of new mMTJs.

4.5. Dystrophin, β-dystroglycan, α-sarcoglycan and merosin

In our study, the expression of dystrophin-associated molecules during regeneration followed the same sequence as has been reported during the development of skeletal muscle [53,54], with the expression of subsarcolemmal proteins preceding that of transmembrane and extracellular proteins. This suggests that during regeneration, the subsarcolemmal proteins play an essential role in the assembly of transmembrane and extracellular components. It may also be interpreted that internal linking of the cytoskeleton to the plasma membrane must be established before the myofibres can be linked to the ECM. In the light of the recently established pivotal role of DG in the assembly of laminin [55], it is logical that the relative increase of β-DG occurred ahead of merosin.

In discordance with our results, Vater et al. [56] reported that β-DG reappeared first during regeneration and was only later followed by dystrophin. It was suggested that ''dystrophin and the glycoprotein complex are synthesized separately, both temporally and spatially, and only become associated at the plasma membrane during the later stages of regeneration.'' Vater et al. [56] used a model of in situ necrosis induced by notexin in which the BM and mysial sheaths remain intact. The presence of preserved BM in in situ necrosis as opposed to disrupted BM in shearing injury

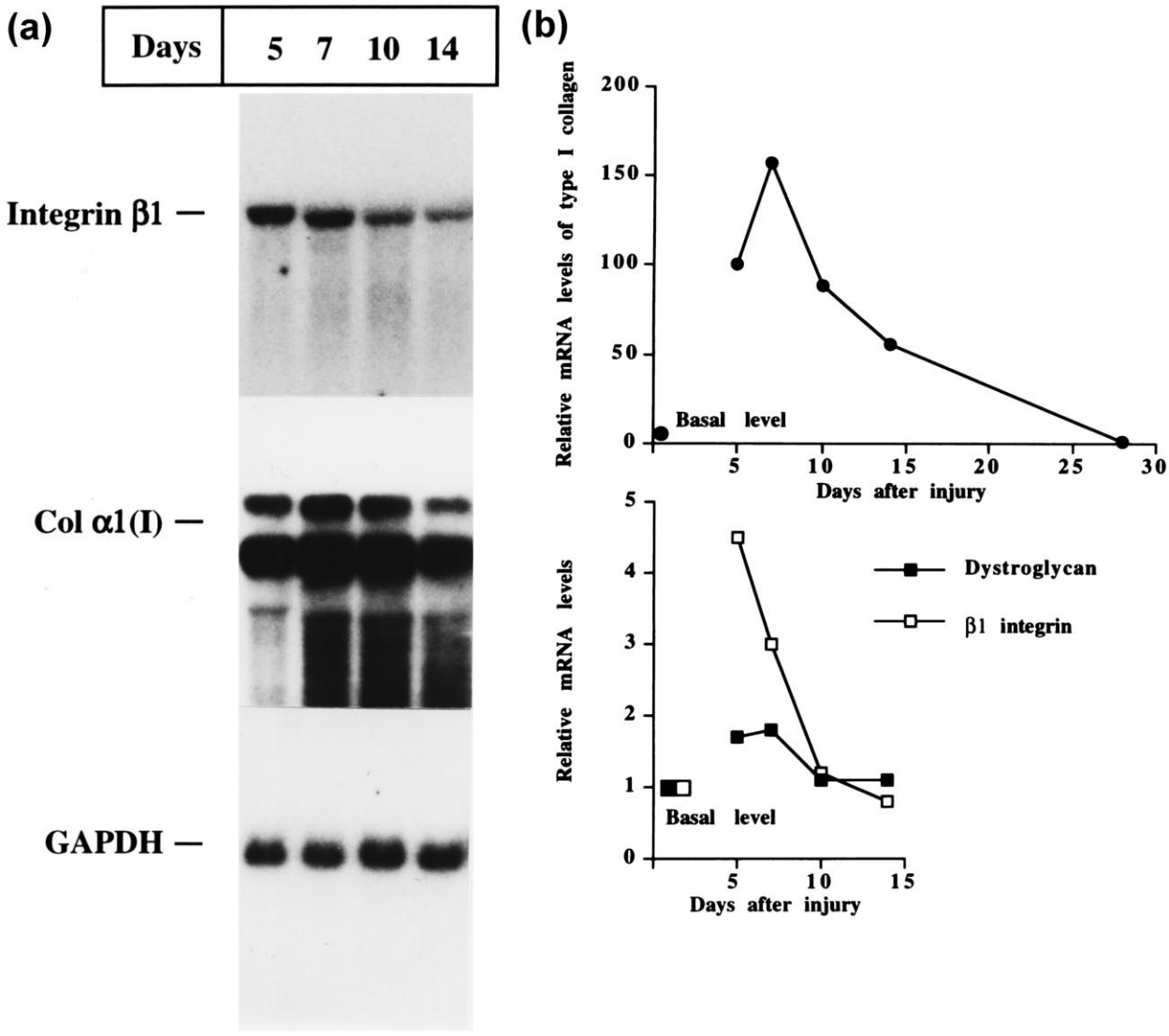

Fig. 10. (a): Northern blots of integrin $\beta 1$ subunit, $\alpha 1$(I) collagen and GAPDH. (b): Quantifications of the Northern blots.

may well modulate the sequence of molecular expression, which possibility is supported by the role ascribed to dystroglycan in BM assembly [55].

The timetables of the expression of integrin and dystrophin associated molecules were markedly different: $\alpha 7$ integrin and vinculin appeared early but after 2 weeks when the intensity of the dystrophin associated molecules increased to remain at a high expression level on the lateral aspects of myofibres, $\alpha 7$ integrin and vinculin were redistributed to the tips of the myofibres. Functionally this may mean that these two complexes of adhesion molecules have complementary roles in myofibre-ECM adhesion. Analogous to this, an enhanced expression of $\alpha 7$ integrin has been reported in disease entities with dystrophin deficiency, i.e. in the muscle of *mdx* mouse and in patients with Duchenne or Becker muscular dystrophy [57]. Muscle of the *mdx* mouse has also been shown to upregulate expression of vinculin [58].

4.6. Correlation between the biomechanical and molecular findings

In our previous study [1] we found that, on pulling, the regenerating muscle ruptured at the scar between the stumps until day 10. During that period the tensile strength of regenerating muscle was rapidly augmented (Fig. 8) and, as shown here, the expressions of $\alpha 7$ integrin and vinculin were enhanced. These molecules most likely contribute to the improved tensile strength, because reinforced lateral adhesion of myofibres reduces the load on the scar tissue overbridging the gap between the stumps and thereby lowers the risk of rerupture and allows use of the injured muscle already before the healing is complete. From day 14 onwards, the pulled muscles failed within myofibres either close to the newly formed mMTJs or next to the original proximal or distal MTJs, the latter being the sites where failure occurs in intact muscles [1]. Thus, after 2 weeks

the distribution and function of the adhesion molecules appear to have attained a more or less normal pattern, although the quantitative normalization and remodelling still continue over a longer period of time.

Acknowledgements

The skilled technical assistance by Ms Liisa Lempiäinen, Ms Heidi Pakarinen and Ms Liisi Salomaa and excellent photographic work by Mr Jaakko Liippo are gratefully acknowledged. This study was supported by grants from the Emil Aaltonen Foundation, The Foundation for Orthopaedical and Traumatological Research in Finland, The Medical Research Funds of Tampere and Turku University Hospitals, The Research Council for Physical Education and Sport, Ministry of Education, Finland, The Juho Vainio Foundation.

References

[1] Kääriäinen M, Kääriäinen J, Järvinen TLN, Sievänen H, Kalimo H, Järvinen M. Correlation between biomechanical and structural changes during the regeneration after laceration injury of skeletal muscle. J Orthop Res 1998;16:197–206.
[2] Kalimo H, Rantanen J, Järvinen M. Muscle injuries in sports. Baillière's Clin Orthop 1997;2:1–24.
[3] Hynes RO. Integrins: A family of cell surface receptors. Cell 1987;48:549–554.
[4] Meredith JE, Winitz S, Lewis JM, Hess S, et al. The regulation of growth and intracellular signaling by integrins. Endocr Rev 1996;17:207–220.
[5] Ruoslahti E, Pirschbacher MD. New perspectives in cell adhesion: RGD and integrins. Science 1987;238:491–497.
[6] Ruoslahti E. Integrins. J Clin Invest 1991;87:1–5.
[7] Brown RH. Dystrophin-associated proteins and the muscular dystrophies: A glossary. Brain Pathol 1996;6:19–24.
[8] Ervasti JM, Campbell KP. Dystrophin and the membrane skeleton. Curr Opin Cell Biol 1993;5:82–87.
[9] Sunada Y, Campbell KP. Dystrophin-glycoprotein complex: molecular organization and critical roles in skeletal muscle. Curr Opin Neurol 1995;8:379–384.
[10] Song WK, Wang W, Foster RF, Bielser DA, Kaufman SJ. H36-α7 is a novel integrin alpha chain that is developmentally regulated during skeletal myogenesis. J Cell Biol 1993;117:643–657.
[11] Otey CA, Pavalko FM, Burridge K. An interaction between α-actinin and the β1 integrin subunit in vitro. J Cell Biol 1990;111:721–729.
[12] Horwitz A, Duggan K, Buck C, Beckerle MC, Burridge K. Interaction of plasma membrane fibronectin receptor with talin – a transmembrane linkage. Nature 1986;320:531–533.
[13] Jockusch BM, Bubeck P, Giehl K, et al. The molecular architecture of focal adhesions. Annu Rev Cell Dev Biol 1995;11:379–416.
[14] Bao ZZ, Lakonishok M, Kaufman S, Horwitz AF. α7β1 Integrin is a component of the myotendinous junction on skeletal muscle. J Cell Sci 1993;106:579–590.
[15] Yao C, Ziober BL, Squillace RM, Kramer RH. α7 integrin mediates cell adhesion and migration on specific laminin isoforms. J Biol Chem 1996;271:15598–25603.
[16] von der Mark H, Dürr J, Sonnenberg A, von der Mark K, Deutzmann R, Goodman SL. Skeletal myoblasts utilize a novel α1-series integrin and not α6β1 for binding to the E8 and T8 fragments of laminin. J Biol Chem 1991;266:23593–23601.
[17] Engvall E, Earwicker D, Haaparanta T, Ruoslahti E, Sanes JR. Distribution and isolation of four laminin variants: tissue restricted distribution of heterotrimers assembled from five different subunits. Cell Regulation 1990;1:731–740.
[18] Engvall E. Laminin variants: why, where and when? Kidney Int 1993;43:2–6.
[19] Ervasti JM, Campbell KP. A role for the dystrophin-glycoprotein complex as a transmembrane linker between laminin and actin. J Cell Biol 1993;122:809–823.
[20] Fabbrizio E, Bonet-Kerrache A, Leger JJ, Mornet D. Actin-dystrophin interface. Biochem 1993;32:10457–10463.
[21] Hemmings L, Kuhlman PA, Critchley DR. Analysis of the actin-binding domain of α-actinin by mutagenesis and demonstration that dystrophin contains a functionally homologous domain. J Cell Biol 1992;116:1369–1380.
[22] Bonilla E, Samitt CE, Miranda AF, et al. Duchenne muscular dystrophy: deficiency of dystrophin at the muscle cell surface. Cell 1988;54:447–452.
[23] Arahata K, Ishiura S, Ishiguro T, et al. Immunostaining of skeletal and cardiac muscle surface membrane with antibody against Duchenne muscular dystrophy peptide. Nature 1988;333:861–863.
[24] Porter GA, Dmytrenko GM, Winkelmann JC, Bloch RJ. Dystrophin colocalizes with α-spectrin in distinct subsarcolemmal domains in mammalian skeletal muscle. J Cell Biol 1992;117:997–1005.
[25] Minetti C, Beltrame F, Marcenaro G, Bonilla E. Dystrophin at the plasma membrane of human muscle fibers shows a costameric localization. Neuromusc Disord 1992;2:99–109.
[26] Yeadon JE, Lin H, Dyer SM, Burden SJ. Dystrophin is a component of the subsynaptic membrane. J Cell Biol 1991;115:1069–1076.
[27] Samitt CE, Bonilla E. Immunocytochemical study of dystrophin at the myotendinous junction. Muscle Nerve 1990;13:493–500.
[28] Byers TJ, Kunkel LM, Watkins SC. The subcellular distribution of dystrophin in mouse skeletal, cardiac, and smooth muscle. J Cell Biol 1991;115:411–421.
[29] Shimizu T, Matsumura K, Sunada Y, Mannen T. Dense immunostainings on both neuromuscular and myotendon junctions with an anti-dystrophin monoclonal antibody. Biomed Res 1989;10:405–409.
[30] Ervasti JM, Campbell KP. Membrane organization of the dystrophin-glycoprotein complex. Cell 1991;66:1121–1131.
[31] Campbell KP, Kahl SD. Association of dystrophin and an integral membrane glycoprotein. Nature 1989;338:259–262.
[32] Yoshida M, Ozawa E. Glycoprotein complex anchoring dystrophin to sarcolemma. J Biochem 1990;108:748–752.
[33] Ervasti JM, Ohlendieck K, Kahl SD, Gaver MG, Campbell KP. Deficiency of a glycoprotein component of the dystrophin complex in dystrophic muscle. Nature 1990;345:315–319.
[34] Yoshida M, Suzuki A, Yamamoto H, Noguchi S, Mizuno Y, Ozawa E. Dissociation of the complex of dystrophin and its associated proteins into several unique groups by n-octyl β-D-glucoside. Eur J Biochem 1994;222:1055–1061.
[35] Wakayama Y, Shibuya S, Takeda A, Jimi T, Nakamura Y, Oniki H. Ultrastructural localization of the C-terminus of the 43-kd dystrophin-associated glycoprotein and its relation to dystrophin in normal murine skeletal myofiber. Am J Pathol 1995;146:189–196.
[36] Suzuki A, Yoshida M, Hayashi K, Mizuno Y, Hagiwara Y, Ozawa E. Molecular organization at the glycoprotein-complex binding site of dystrophin; three dystrophin-associated proteins bind directly to the carboxyl-terminal portion of dystrophin. Eur J Biochem 1994;220:283–292.
[37] Ibraghimov-Beskrovnaya O, Ervasti JM, Leveille CJ, Slaughter CA, Sernett SW, Campbell KP. Primary structure of dystrophin-associated glycoproteins linking dystrophin to the extracellular matrix. Nature 1992;355:696–702.{oφ
[38] Sunada Y, Bernier SM, Kozak CA, Yamada Y, Campbell KP. Deficiency of merosin in dystrophic dy mice and genetic linkage of laminin M chain gene to dy locus. J Biol Chem 1994;269:13729–13732.
[39] Bland JM, Altman DG. Measurement: Statistical methods for asses-

sing agreement between two methods of clinical measurement. Lancet 1986;i:307–310.

[40] Chirgwin JM, Przybyla AE, McDonald RJ, Rutter WJ. Isolation of biologically active ribonucleic acid from sources enriched in ribonuclease. Biochem 1979;18:5294–5299.

[41] Genovese C, Rowe D, Kream B. Construction of DNA sequences complementary to rat α1 and α2 collagen mRNA and their use in studying the regulation of type I collagen synthesis by 1,25-dihydroxyvitamin D. Biochem 1984;23:6210.

[42] Fort PL, Marty L, Piechaczyk M, et al. Various rat adult tissues express only one major mRNA species from the glyceraldehyde-3-phosphate-dehydrogenase multigenic family. Nucl Acids Res 1985;13:1431–1442.

[43] Hurme T, Kalimo H, Lehto M, Järvinen M. Healing of skeletal muscle injury: an ultrastructural and immunohistochemical study. Med Sci Sports Exerc 1991;23:801–810.

[44] Järvinen M. Healing of a crush injury in rat striated muscle: 2 A histological study of the effect of early mobilization and immomobilization on the repair process. Acta Path Microbiol Scand A 1975;83:269–282.

[45] Lehto M, Sims TJ, Bailey AJ. Skeletal muscle injury – molecular changes in the collagen during healing. Res Exp Med 1985;185:95–106.

[46] Hurme T, Kalimo H, Sandberg M, Lehto M, Vuorio E. Localization of type I and III collagen and fibronectin production in injured gastrocnemius muscle. Lab Invest 1991;64:76–84.

[47] Tidball JG, Daniel TL. Myotendinous junctions of tonic muscle cells: Structure and loading. Cell Tissue Res 1986;245:315–322.

[48] Tidball JG. Force transmission across muscle membrane. J Biomech 1991;24(Suppl 1):43–52.

[49] Heino J, Ignotz RA, Hemler ME, Crouse C, Massagne J. Regulation of cell adhesion receptors by transforming growth factor-β. Concomitant regulation of integrins that share a common β1 subunit. J Biol Chem 1989;264:380388.

[50] Hurme T, Kalimo H. Adhesion in skeletal muscle during regeneration. Muscle Nerve 1992;15:482–489.

[51] Kami K, Masuhara M, Kashiba H, Kawai Y, Noguchi K, Senba E. Changes of vinculin and extracellular metrix components following blunt trauma to rat skeletal muscle. Med Sci Sports Exerc 1993;25:832–840.

[52] Felsenfeld DP, Choquet D, Sheetz MP. Ligand binding regulates the directed movement of β1 integrins on fibroblasts. Nature 1996;383:438–440.

[53] Mora M, Blasi CD, Barresi R, et al. Developmental expression of dystrophin, dystrophin-associated glycoproteins and other membrane cytoskeletal proteins in human skeletal and heart muscle. Dev Brain Res 1996;91:70–82.

[54] Tomè FMS, Matsumura K, Chevalley M, Campbell KP, Fardeau M. Expression of dystrophin-associated glycoproteins during human fetal muscle development. A preliminary immunocytochemical study. Neuromusc Disord 1994;4:343–348.

[55] Henry MD, Campbell KP. A role for dystroglycan in basement membrane assembly. Cell 1998;11:859–870.

[56] Vater R, Harris JB, Anderson LVB, Roberds SL, Campbell KP, Cullen MJ. The expression of dystrophin-associated glycoproteins during skeletal muscle degeneration and regeneration. An immunofluorescence study. J Neuropathol Exp Neurol 1995;54:557–569.

[57] Hodges BL, Hayashi YK, Nonaka I, Wang W, Arahata K, Kaufman SJ. Altered expression of the α7β1 integrin in human and murine muscular dystrophies. J Cell Sci 1997;110:2873–2881.

[58] Law DJ, Allen DL, Tidball JG. Talin, vinculin and DRP (utrophin) concentrations are increased at mdx myotendinous junctions following onset of necrosis. J Cell Sci 1994;107:1477–1483.